GL-TR-89-0177





# Polar Bear UV Images of Airglow and Aurora- Data Reduction and Analysis

Moshe Tur
Israel Oznovich

Tel Aviv University/RAMOT Ltd
Faculty of Engineering
Ramot Aviv
Tel Aviv 69978, ISRAEL

29 September 1988

Scientific Report No. 1

APPROVED FOR PUBLIC RELEASE; DISTRIBUTION UNLIMITED



GEOPHYSICS LABORATORY
AIR FORCE SYSTEMS COMMAND
UNITED STATES AIR FORCE
HANSCOM AIR FORCE BASE, MASSACHUSETTS 01731-5000

"This technical report has been reviewed and is approved for publication"

F.P DelGreco

FRANCIS P. DEL GRECO
Contract Manager

Robert E. Huffman

ROBERT E. HUFFMAN
Branch Chief

FOR THE COMMANDER

H Carlson

HERBERT C. CARLSON, Acting Director
Ionospheric Physics Division

This report has been reviewed by the ESD Public Affairs Office (PA) and is releasable to the National Technical Information Service (NTIS).

Qualified requestors may obtain additional copies from the Defense Technical Information Center. All others should apply to the National Technical Information Service.

If your address has changed, or if you wish to be removed from the mailing list, or if the addressee is no longer employed by your organization, please notify AFGL/DAA, Hanscom AFB, MA 01731. This will assist us in maintaining a current mailing list.

Do not return copies of this report unless contractual obligations or notices on a specific document requires that it be returned.

Unclassified

SECURITY CLASSIFICATION OF THIS PAGE

# REPORT DOCUMENTATION PAGE

| | |
|---|---|
| 1a. REPORT SECURITY CLASSIFICATION<br>Unclassified | 1b. RESTRICTIVE MARKINGS |
| 2a. SECURITY CLASSIFICATION AUTHORITY | 3. DISTRIBUTION / AVAILABILITY OF REPORT<br>Approved for public release;<br>Distribution unlimited |
| 2b. DECLASSIFICATION / DOWNGRADING SCHEDULE | |
| 4. PERFORMING ORGANIZATION REPORT NUMBER(S) | 5. MONITORING ORGANIZATION REPORT NUMBER(S)<br>GL-TR-89-0177 |
| 6a. NAME OF PERFORMING ORGANIZATION<br>Tel Aviv University/RAMOT Ltd<br>6b. OFFICE SYMBOL (If applicable) | 7a. NAME OF MONITORING ORGANIZATION<br>European Office of Aerospace Research and Development |
| 6c. ADDRESS (City, State, and ZIP Code)<br>Faculty of Engineering<br>Ramot Aviv, Tel Aviv 69978 ISRAEL | 7b. ADDRESS (City, State, and ZIP Code)<br>Box 14<br>FPO New York 09510-0200 |
| 8a. NAME OF FUNDING / SPONSORING ORGANIZATION<br>Geophysics Laboratory<br>8b. OFFICE SYMBOL (If applicable)<br>LIU | 9. PROCUREMENT INSTRUMENT IDENTIFICATION NUMBER<br>F49620-87-C-0091 |
| 8c. ADDRESS (City, State, and ZIP Code)<br>Hanscom AFB<br>Massachusetts 01731-5000 | 10. SOURCE OF FUNDING NUMBERS<br>PROGRAM ELEMENT NO: 62101F; PROJECT NO: 4643; TASK NO: 11; WORK UNIT ACCESSION NO: AB |

11. TITLE (Include Security Classification)
Polar Bear UV Images of Airglow and Aurora - Data Reduction and Analysis

12. PERSONAL AUTHOR(S)
Moshe Tur, Israel Oznovich

| 13a. TYPE OF REPORT | 13b. TIME COVERED | 14. DATE OF REPORT (Year, Month, Day) | 15. PAGE COUNT |
|---|---|---|---|
| Scientific #1 | FROM Sep 87 TO Sep 88 | 1988 September 29 | 38 |

16. SUPPLEMENTARY NOTATION

| 17. COSATI CODES | | |
|---|---|---|
| FIELD | GROUP | SUB-GROUP |
| | | |
| | | |

18. SUBJECT TERMS (Continue on reverse if necessary and identify by block number)
Aurora
Airglow
Ultraviolet
Image processing

19. ABSTRACT (Continue on reverse if necessary and identify by block number)

The AIRS scanning ultraviolet photometer aboard the Polar Bear satellite was launched in late 1986. It was designed to obtain UV images with high spatial and wavelength resolution at several emission lines simultaneously. The objective of the program is to geometrically and photometrically calibrate the data. The processing is designed to provide kilometer-scaled images that can be projected upon various coordinate systems. These tools afford studies of the spatial and temporal variability of airglow and aurora.

Each data-stream from a pass is converted to a 240 x 240 image representing 5000 x 5000km records of intensity. The major progress during the report period has been modification and development of programs to accomplish the following:

1) A Chapman function correction to the solar flux dependence of the intensity, resulting with a successful daytime fit of power unity of above variable to pixel brightness.

2) Separation of night-glow domain to ordinary and continuous (24 hr) night regions.

3) Projection of images onto dipole & corrected geomagnetic coordinate systems.

4) Comparison of auroral arcs with known auroral oval and initiation of a UV oval→(OVER)

| | |
|---|---|
| 20. DISTRIBUTION / AVAILABILITY OF ABSTRACT<br>☐ UNCLASSIFIED/UNLIMITED ☐ SAME AS RPT ☐ DTIC USERS | 21. ABSTRACT SECURITY CLASSIFICATION<br>Unclassified |
| 22a. NAME OF RESPONSIBLE INDIVIDUAL<br>Frank DelGreco | 22b. TELEPHONE (Include Area Code) / 22c. OFFICE SYMBOL<br>GL/LIU |

DD FORM 1473, 84 MAR 83 APR edition may be used until exhausted
All other editions are obsolete.

SECURITY CLASSIFICATION OF THIS PAGE
Unclassified

CONT OF BLOCK 19:

from input images.

Contents

## 1. Research Goals

The overall objective of the effort in Far UV ionospheric imaging is to relate Far UV intensities together with in-situ measurements of ion density and temperature to deduce near real-time electron-density profiles. This data will be used in conjunction with ground-based ionosonde data and total electron content to specify the global EDP for C3I system users.

The principal objective of this research is to photometrically and geometrically process UV satellite images and develop models which describe these observations in terms of photochemical and geophysical mechanisms.

a) Develop image proceesing algorithms to convert Polar Bear satellite records of intensity versus time to images.

b) Geometrically process the data to correct for satellite roll and orientation; locate limb brightening of optically thin emission lines.

c) Apply photometric corrections such as incident solar flux and column path length to obtain a nadir-viewing image; the goal is to achieve a consistent analysis scheme based on first principles to match day and night observations.

d) Project each image onto its relevant geographic and geomagnetic coordinates.

e) Separate aurora from airglow; cross-correlate auroral morphology spectroscopically and temporally.

## 2. Introduction

The USAF Geophysics Lab has developed and flown the first instrumentation designated for UV imagery with high spatial and wavelength resolution. The AIM scanner flown on the HILAT satellite provided the earliest data showing airglow and auroral morphology and emission processes. HILAT returned a number of images in 1983 with a 30A spectral resolution and 5x20 km spatial resolution. The AIM instrumentation aboard HILAT has been described in several references ( 1, 2, 3, and 4).

In late 1986, AFGL launched a second satellite with similar instrumentation. The Polar Bear satellite is designated for UV imagery with high spatial and wavelength resolution. The satellite carries the AIRS scanning ultraviolet photometer providing several simultaneous spectral images, representing the integrated column photon count of several different upper - atmosphere species. The data stream is currently converted to 240 line x 240 column images representing 5000 km x 5000 km records of intensity.

Prof. Norman Rosenberg has laid the foundations for the photometric and geometric processing of both the AIM and the AIRS instruments (ref. 5, and 6). This research was lately struck by the untimely death of Prof. Rosenberg. The continuation of the research was afforded to us based on the formidable work and progress achieved by the late Rosenberg.

A software package has been developed to process large number of images supplied by the AIRS instrument. This package transforms the time-spaced data stream to a photometrically - standardized image which is linearly kilometer-scaled.

Table 1 presents a summary of programs newly developed or updated during the report period. A data-flow diagram for basic image processing of the AIRS pictures is shown in Table 2. The flowsheet shows processes, and input and output files generated for a given scene and detector. A scene NN is defined as a multi-detector record for a given site, day, and pass. Note that for every scene processing, programs rawcvt and scene need be applied just once, as files hdrNN.d, geoNN.d, and selNN.i are common to all detectors within that scene.

Table 1

| Program | Type | Description |
|---|---|---|
| amov | util | automatic move-image procedure |
| aurmean | air | northern-hemisphere UV auroral oval |
| aurplot | air | plot image upon geomagenetic coordinate system |
| chapman | util | Chapman function Ch(x,X) for -15<=selv<=25 degrees |
| corrgm | util | corrected geomagnetic lat lon for geographic lat lon |
| detc | air | smooth, amplify, filter, and warp raw image |
| dipgm | util | dipole geomagnetic lat lon for geographic lat lon |
| distance | img | distance image of object to background for given image |
| geomlsq | air | seperate aurora from airglow |
| gmcoord | air | overlay geographic/geomagnetic grid upon image |
| grafim | img | graph histogram or average brightness on screen |
| landmass | air | geographic grid and/or landmass features on image |
| line | util | draw line on screen |
| monthday | util | month and day from year and day number |
| mulbnd | img | two-color output image from two input detectors |
| pl_graf | util | plot any integer vector y versus vector x on screen |
| plotgm | util | draw geomagnetic grid upon image via given geographic lat lon coordinates |
| rawcvt | air | convert raw diskette to image file |
| replsq | air | report least-squares fit data for many images |
| rhline_pc | img | emulate pc integer size to vax int size |
| rhline_vax | img | emulate FG100AT procedures to IP-512 software |
| scene | air | orbit, geometrical, and geophysical parameters |
| stdsubs | util | standard subroutines |
| sundec | util | sun declination from date and time |
| tchap | util | test Chapman function routine |
| xmov | img | move image from qd to qd, from disk to qd, or from qd to disk file |

Table 2

| INPUT Data | INPUT Images | PROCESS | OUTPUT Data | OUTPUT Images |
|---|---|---|---|---|
| S87dateD.d | | -> rawcvt | -> rawNN.d | rawNND.1 |
| rawNN.d | rawNND.1 | -> scene | -> hdrNN.d<br>geoNN.d | selNN.1 |
| hdrNN.d<br>geoNN.d | rawNND.1 | -> detc | -> hdrNN.d | warpNND.1 |
| hdrNN.d | selNN.1<br>warpNND.1 | -> geomlsq | -> hdrNN.d<br>lsqNND.d | aurNND.1 |

## 3. Data Sources

The Polar Bear satellite cruises at an altitude of approximately 1000 kilometers at an inclination angle of 89.56 degrees to the equator, i.e. in a polar-to-polar orbit.

The AIRS scanner provides 326 samples of emission count in an angular scan from -65 to +65 degrees perpendicular to the satellite orbit. The scan cycle is completed in 3 seconds and a typical 11 minute recording provides c220 scan lines. Since the satellite cruises at a ground velocity of 6.3 kms/sec, each scan line is about 20 ground kilometers ahead of the previous line.

Because the satellite platform is not well stabilized, pitch, yaw, and roll corrections to the scan pointing direction must be included. In general scan lines were not parallel, and did not lie along a line perpendicular to the orbital ground path.

The warped image was scaled to fit a 240 x 240 pixel map representing 5000 x 5000 km by interpolating raw count values from the scanner angle image to this kilometer image.

Seven detectors are installed on the AIRS instrument. They are listed in Table 3 with their sensitivities (in Rayleighs per count), and wavelengths in Angtroms.

Table 3

| detector | wavelength | sensitivity |
|---|---|---|
| 1 | 1596 | 90 |
| 2 | 1356 | 30 |
| 3 | 3914 | 320 |
| 4 | 1733 | 230 |
| 5 | 1493 | 45 |
| 6 | 1544 | 75 |
| 7 | 1304 | 25 |

## 4. Geometric Processing

### 4.1 RAWCVT -

Convert a raw ASCII diskette file containing about 220 lines taken over 660 seconds into a 240 line x 240 column binary image, and an orbital data file. The program handles data gaps and tests wether the raw data is packed. If packed, program UNPAK is invoked to generate a non-saturated image.

The program's HELP utility appears in appendix 1a. An example of a pre and post - processed image by rawcvt is shown in Figure 1.

### 4.2 SCENE - contains rawfit, roladj, geomim, solel, and part of warpim

The program handles a single scene (common to all three detectors) to produce the followig :

(1) a common header file (hdrNN.d);
(2) a geographic data file (geoNN.d) containing satellite orbital data, image x and y ground coordinates, and angles to the horizon;
(3) an image file (selNN.i) containing the following geophysical parameters :
    a. inverse path length.
    b. corrected sine(solar elevation). ( * )
    c. number of hours since sunset/sunrise at raw time.
    d. total daily solar exposure time, in hours.

(*) The correction to the sine(selv) value, both positive and negative, was performed due to failure of the plane parallel approximation at low elevation angles ( dip <= selv <= 25 degrees, where dip is the 150km UV sunset/sunrise dip angle ). We used Chapman function Ch(x,X) values using a scale height gradient of 0.75 at 150 km (ref. 7, 8 and 9). Ch(x,X) is the modified Chapman function. Variable x is the solar zenith angle ( x = 90 - selv ), and X = (R+h)/H(0) = 170, where H(0) = 38.4 km is the atomic oxygen scale height at 150 km.

Figure 2 presents a typical scene processing. Figure 2a is the chosen raw image for roll adjustment. The choice is centered on the most sensitive detector available. The roll adjustment algorithm is exemplified on an amplified and differentiated image in Figure 2b. The four geophysical variables discussed above are imaged in Figure 2c.

Help utility for scene appears in appendix 1b. Also presented are typical scene output meassages and file contents.

Table 4 presents sin(selv) versus Chapman function values for solar elevation angles -10 to 25 degrees. At selv = 25 degrees there is a 5% difference between the values of the two functions. We interpolated between these two functions in the range of selv=25 to selv=20 degrees to assure continuity. Sin(selv) is obviously undefined at geometrical zenith angles >= 90 degrees.

Table 4 column headings are :

| | | |
|---|---|---|
| selv | - | solar elevation angle in degrees |
| zenith | - | zenith angle = 90 - selv |
| chapf | - | modified chapman function Ch(x,X) |
| sin(selv) | - | sine(solar elevation) |
| % err | - | percent error |

Table 4

| selv | zenith | chapf | sin(selv) | % err | 1/chap | 1/sin(selv) | % err |
|---|---|---|---|---|---|---|---|
| 25.0 | 65.0 | 0.42 | 0.42 | 0.0% | 2.37 | 2.37 | 0.0% |
| 24.0 | 66.0 | 0.41 | 0.41 | 1.1% | 2.43 | 2.46 | 1.2% |
| 23.0 | 67.0 | 0.40 | 0.39 | 2.4% | 2.50 | 2.56 | 2.5% |
| 22.0 | 68.0 | 0.39 | 0.37 | 3.9% | 2.57 | 2.67 | 4.1% |
| 21.0 | 69.0 | 0.38 | 0.36 | 5.5% | 2.64 | 2.79 | 5.9% |
| 20.0 | 70.0 | 0.37 | 0.34 | 7.3% | 2.71 | 2.92 | 7.9% |
| 19.0 | 71.0 | 0.35 | 0.33 | 8.0% | 2.83 | 3.07 | 8.7% |
| 18.0 | 72.0 | 0.34 | 0.31 | 8.6% | 2.96 | 3.24 | 9.5% |
| 17.0 | 73.0 | 0.32 | 0.29 | 9.4% | 3.10 | 3.42 | 10.4% |
| 16.0 | 74.0 | 0.31 | 0.28 | 10.2% | 3.26 | 3.63 | 11.4% |
| 15.0 | 75.0 | 0.29 | 0.26 | 11.2% | 3.43 | 3.86 | 12.6% |
| 14.0 | 76.0 | 0.28 | 0.24 | 12.3% | 3.62 | 4.13 | 14.1% |
| 13.0 | 77.0 | 0.26 | 0.22 | 13.6% | 3.84 | 4.45 | 15.7% |
| 12.0 | 78.0 | 0.25 | 0.21 | 15.2% | 4.08 | 4.81 | 17.9% |
| 11.0 | 79.0 | 0.23 | 0.19 | 16.7% | 4.36 | 5.24 | 20.1% |
| 10.0 | 80.0 | 0.21 | 0.17 | 18.7% | 4.68 | 5.76 | 23.0% |
| 9.0 | 81.0 | 0.20 | 0.16 | 21.0% | 5.05 | 6.39 | 26.6% |
| 8.0 | 82.0 | 0.18 | 0.14 | 23.8% | 5.48 | 7.19 | 31.2% |
| 7.0 | 83.0 | 0.17 | 0.12 | 27.2% | 5.97 | 8.21 | 37.4% |
| 6.0 | 84.0 | 0.15 | 0.10 | 31.3% | 6.57 | 9.57 | 45.6% |
| 5.0 | 85.0 | 0.14 | 0.09 | 36.5% | 7.29 | 11.47 | 57.4% |
| 4.0 | 86.0 | 0.12 | 0.07 | 43.0% | 8.17 | 14.34 | 75.5% |
| 3.0 | 87.0 | 0.11 | 0.05 | 51.5% | 9.28 | 19.11 | 106.0% |
| 2.0 | 88.0 | 0.09 | 0.03 | 62.7% | 10.70 | 28.65 | 167.9% |
| 1.0 | 89.0 | 0.08 | 0.02 | 78.1% | 12.57 | 57.30 | 355.7% |
| 0.0 | 90.0 | 0.07 | 0.00 | 100.0% | 15.15 | 0.00 | 0.0% |
| -1.0 | 91.0 | 0.05 | -0.02 | 133.2% | 19.00 | 0.00 | 0.0% |
| -2.0 | 92.0 | 0.04 | -0.03 | 178.2% | 22.40 | 0.00 | 0.0% |
| -3.0 | 93.0 | 0.03 | -0.05 | 251.3% | 28.90 | 0.00 | 0.0% |
| -4.0 | 94.0 | 0.03 | -0.07 | 354.6% | 36.50 | 0.00 | 0.0% |
| -5.0 | 95.0 | 0.02 | -0.09 | 483.5% | 44.00 | 0.00 | 0.0% |
| -6.0 | 96.0 | 0.02 | -0.10 | 601.7% | 48.00 | 0.00 | 0.0% |
| -7.0 | 97.0 | 0.02 | -0.12 | 806.8% | 58.00 | 0.00 | 0.0% |
| -8.0 | 98.0 | 0.01 | -0.14 | 1032.5% | 67.00 | 0.00 | 0.0% |
| -9.0 | 99.0 | 0.01 | -0.16 | 1210.7% | 71.00 | 0.00 | 0.0% |
| -10.0 | 100.0 | 0.01 | -0.17 | 1419.7% | 76.00 | 0.00 | 0.0% |

## 5. Photometric Processing

### 5.1 DETC - contains a new filtraw, and part of warpim

The program handles one detector out of three that belong to a certain scene. Its final output is in the form of an image (warpNND.1), corrected geometrically and rescaled photometrically. It also updates the header file hdrNN.d with the amplification, and the raw percent aurora.

The new filtering routine does the following :
(1) smoothes noise via most-frequent value method;
(2) finds percent aurora in image: ( ** )
(3) apmlifies and filters the image.

(**) The algorithm I developed and currently use is a statistical one. It basically builds a crude block-like model of the image based on surround statistics to predict the percent aurora in the image.

Figure 3a shows a raw image on which detc works. It creates a crude auroral model, shown in Fig. 3b. This model enables an estimate of pcau - percent aurora in the image.

The two filters, narrow and wide, used by filtraw are shown in Figure c and 3d respectively. The output image on Fig. 3e, amplified and smoothed, is a combination of the two images in Figures 3c and 3d. The warped image, being the final output of detc, is shown in Fig. 3f.

The program's Help utility, and typical DETC output parameters appear in appendix 2a.

### 5.2 GEOMLSQ

Fit various geophysical parameters to the geometrically corrected image in order to seperate aurora from airglow.

The least-squares fit is performed on the brightness b of a pixel as a function of inverse path length p, and the corrected sin(selv) s to produce coefficients C0, C1, and C2 in the following domains :

(1) daylight: b = C0 * (p** C1) * (s** C2)
(2) night: b = C0 * (p** C1)
(3) continous night: b = C0 * (p** C1)
where continous (24 hr) night is the boreal winter night.

Geomlsq uses the coefficients found to compare actual and expected brightness in every pixel. A criteria of actual/expected intensity, in conjunction with an auroral brightness threshold, are used to distiguish airglow from auroral pixels.

Help utility for geomlsq appears in appendix 2b. File hdrNN.d is updated, and file lsqNND.d created to report lsq fit results. The program uses the warped image shown in Figure 4a, and the geophysical parameters (Fig. 4b) to produce a final auroral image (Fig. 4c). An image that compares the fitted intensity values with the actual ones is also provided. Figure 4d has an intensity of 100 * (actual br/expected br). Two boundary regions are marked in Fig. 4d - sunset/sunrise line, and boreial winter border.

## 6. Coordinate Systems

### 6.1 LANDMASS

Plot geographic grid and/or landmass features upon the warped image.

Figures 5, 6, and 7 present coordinate systems applied to auroral images by landmass, aurplot, and gmcoord respectively. The detailed results of aurmean are discussed in section 7.2.

### 6.2 AURPLOT

(1) Plots auroral image upon geomagnetic dipole coordinate system, or upon geomagnetic corrected dipole coordinate system.
(2) Overlay Feldstein's auroral oval (geomagnetic index Q=3) on above images (ref. 9, 10, and 11).
(3) Rotate coordinate systems according to geomagnetic-time corresponding image acquisition time, i.e. both image and coordinate system's geomagnetic noon points up.

6.3 GMCOORD

Plot geographic, corrected, or dipole geomagnetic coordinates upon warped auroral image (aurNND.1). This program is similar to aurplot, and based on the same algorithm, with an inverse interpolation approach.

6.4 AURMEAN

(1) Plot a 240x240 auroral image upon a 512x512 geomagnetic dipole system, or geomagnetic corrected dipole cordinate system.
(2) Rotate image to have geomagnetic noon point up.
(3) Average current image with previously processed auroras in northern geomagnetic hemisphere.

AURMEAN adds-up auroral images by aligning and rotating them (1 and 2) to the same coordinate system. Then it rescales each image intensity by dividing each pixel's brightness by the proper amplification applied to the raw image by program DETC. Averaging of the images to creat a final one is done on a pixel-to-pixel basis. Thus the intensity of a pixel in the final image is a sum of intesities from all normalized images divided by the number of images which include this specific area. This method of averaging produces an overall map of auroral occurrence in the northern hemisphere in the UV for every detector.

Help utilities for above four programs, and typical output meassages are listed in appendix 3.

## 7. Results and Conclusions

### 7.1 Airglow

Table 5 presents a summary of geomlsq results on 13 scenes, as prepared by replsq.

Table column headings are :

| | |
|---|---|
| illum | illumination domain - day, night, or continous night |
| scene | scene number |
| day | day number |
| lmt | local mean time |
| amp | amplification factor |
| pcsl | percent sunlit |
| pcau | percent aurora |
| C01 | count in amplified filtered image, normalized to unit path length and zero zenith distance (selv=90 degrees) |
| Cp | path length power |
| Cs | corrected sine(solar elevation) power |
| sg0 | standard deviation of input points in log10 units |
| pcvf | percent of variance remaining after fit |
| pcvx | percent of variance remaining after fit forcing Cp=1, Cs=1 |
| Ray | Rayleigh count normalized from C01, corrected for amplification and detector sensitivity |

Note that if pcvx is close to pcvf, the forced fit is as valid as the free fit.

Also Note that if pcvr is above 50%, data scatter is so high that there is no significant dependence on the parameters. In order to highlight results from successful fits, we created table 6. Table 6 is similar to table 5, yet presents parameters for those fits whose pcvr is less than or equals 50% only.

Some of the interesting results we have been getting from geomlsq lately concern the corrected sin(selv), and the new parameters in selNN.1. Recall that Bob found a power dependence of the brightness on inverse path length of -1 and sin(selv) of 0.5. Values of sin(selv) differ appreciably ( > 10% ) from the Chapman-corrected sin(selv) values at low solar elevation angles ( see Table 4). We have come-up with a power dependence of 1 for this parameter in all the images we fitted until now (see Table 6). This seem to better conform with the basic physics of the emission process.

One may observe from Table 5 that the fit of brightness b = C0*(p**C1)*(s**C2) to path length p and corrected sin(selv) s with C1 = C2 = 1 was highly successful in the daytime. It was poor during nighttime, both in normal and in continous (the boreial winter) dark hours. We suspect the extremely low count rate from nightglow emission may posses an insufficient signal to noise ratio for a detailed fit as such.

Nevertheless, in the future we plan to investigate possible nightly emission fall-off with time since sunset. At least one of the working detectors (det 2 - 1356 A) may posses the required sensitivity for the fit.

Table 5

det = 1 wvl = 1596 A

| illum | scene | day | lmt | amp | pcsl | pcau | C01 | Cp | Cs | sg0 | pcvf | pcvx | Ray |
|---|---|---|---|---|---|---|---|---|---|---|---|---|---|
| day | 02 | 23 | 11.5 | 85.0 | 67 | 16 | 106.1 | 0.95 | 1.03 | 0.22 | 27 | 30 | 112 |
| day | 03 | 23 | 11.5 | 127.5 | 51 | 54 | 152.2 | 0.63 | 0.69 | 0.22 | 72 | 80 | 107 |
| day | 04 | 42 | 10.2 | 85.0 | 91 | 15 | 97.6 | 0.89 | 0.95 | 0.23 | 24 | 27 | 103 |
| day | 05 | 43 | 10.1 | 85.0 | 73 | 12 | 59.8 | 0.91 | 0.49 | 0.21 | 30 | 36 | 63 |
| day | 06 | 47 | 9.9 | 51.0 | 75 | 20 | 60.3 | 0.81 | 0.95 | 0.21 | 17 | 21 | 106 |
| day | 07 | 48 | 9.8 | 85.0 | 79 | 25 | 108.5 | 0.85 | 0.98 | 0.24 | 34 | 37 | 114 |
| day | 08 | 55 | 9.3 | 63.8 | 82 | 22 | 85.1 | 0.76 | 0.81 | 0.23 | 38 | 43 | 12 |
| night | 05 | 43 | 10.1 | 85.0 | 73 | 12 | 2.5 | 0.99 | 0.00 | 0.09 | 43 | 0 | 2 |
| night | 06 | 47 | 9.9 | 51.0 | 75 | 20 | 2.2 | 0.98 | 0.00 | 0.12 | 60 | 0 | 3 |
| night | 07 | 48 | 9.8 | 85.0 | 79 | 25 | 1.9 | 2.57 | 0.00 | 0.39 | 14 | 0 | 2 |
| night | 08 | 55 | 9.3 | 63.8 | 82 | 22 | 2.2 | 1.03 | 0.00 | 0.11 | 43 | 0 | 3 |
| night | 11 | 25 | 23.5 | 127.5 | 0 | 95 | 6.7 | 0.70 | 0.00 | 0.32 | 85 | 0 | 4 |
| night | 12 | 24 | 23.6 | 85.0 | 0 | 114 | 13.2 | -0.51 | 0.00 | 0.33 | 92 | 0 | 13 |
| night | 13 | 29 | 23.3 | 28.3 | 0 | 72 | 16.1 | -0.70 | 0.00 | 0.42 | 91 | 0 | 51 |
| night | 14 | 32 | 23.0 | 51.0 | 0 | 72 | 10.0 | 0.77 | 0.00 | 0.51 | 92 | 0 | 17 |
| night | 15 | 43 | 22.3 | 36.4 | 0 | 87 | 28.6 | -0.78 | 0.00 | 0.52 | 92 | 0 | 70 |
| ctnit | 02 | 23 | 11.5 | 85.0 | 67 | 16 | 3.4 | 1.60 | 0.00 | 0.21 | 26 | 0 | 3 |
| ctnit | 03 | 23 | 11.5 | 127.5 | 51 | 54 | 8.1 | 0.52 | 0.00 | 0.23 | 91 | 0 | 5 |
| ctnit | 05 | 43 | 10.1 | 85.0 | 73 | 12 | 4.3 | 0.02 | 0.00 | 0.09 | 100 | 0 | 4 |
| ctnit | 06 | 47 | 9.9 | 51.0 | 75 | 20 | 3.0 | 1.00 | 0.00 | 0.09 | 75 | 0 | 5 |
| ctnit | 07 | 48 | 9.8 | 85.0 | 79 | 25 | 4.8 | -1.17 | 0.00 | 0.12 | 83 | 0 | 5 |
| ctnit | 08 | 55 | 9.3 | 63.8 | 82 | 22 | 2.1 | 3.86 | 0.00 | 0.05 | 64 | 0 | 2 |
| ctnit | 11 | 25 | 23.5 | 127.5 | 0 | 95 | 4.6 | -1.04 | 0.00 | 0.10 | 92 | 0 | 3 |
| ctnit | 12 | 24 | 23.6 | 85.0 | 0 | 114 | 16.8 | -3.53 | 0.00 | 0.30 | 47 | 0 | 17 |

det = 2  wvl = 1356 A

| illum | scene | day | lmt | amp | pcsl | pcau | C01 | Cp | Cs | sg0 | pcvf | pcvx | Ray |
|---|---|---|---|---|---|---|---|---|---|---|---|---|---|
| day | 02 | 23 | 11.5 | 7.3 | 68 | 8 | 128.5 | 0.90 | 0.85 | 0.18 | 4 | 6 | 528 |
| day | 03 | 23 | 11.5 | 10.2 | 58 | 18 | 229.7 | 0.82 | 0.99 | 0.16 | 9 | 14 | 675 |
| day | 04 | 42 | 10.2 | 6.7 | 91 | 8 | 114.1 | 0.93 | 0.98 | 0.21 | 3 | 4 | 510 |
| day | 05 | 43 | 10.1 | 7.3 | 74 | 7 | 90.1 | 0.96 | 0.80 | 0.20 | 6 | 6 | 370 |
| day | 06 | 47 | 9.9 | 5.7 | 75 | 14 | 140.4 | 0.89 | 1.21 | 0.22 | 2 | 3 | 742 |
| day | 07 | 48 | 9.8 | 6.5 | 78 | 16 | 110.9 | 0.96 | 1.02 | 0.21 | 5 | 5 | 508 |
| day | 08 | 55 | 9.3 | 6.4 | 81 | 12 | 93.4 | 0.92 | 0.82 | 0.21 | 4 | 5 | 439 |
| night | 07 | 48 | 9.8 | 6.5 | 78 | 16 | 1.6 | 2.65 | 0.00 | 0.31 | 21 | 0 | 7 |
| night | 11 | 25 | 23.5 | 18.2 | 0 | 104 | 13.3 | 0.35 | 0.00 | 0.32 | 97 | 0 | 21 |
| night | 12 | 24 | 23.6 | 11.1 | 0 | 86 | 27.2 | -1.17 | 0.00 | 0.48 | 79 | 0 | 73 |
| night | 13 | 29 | 23.3 | 4.4 | 0 | 58 | 25.0 | -0.76 | 0.00 | 0.43 | 90 | 0 | 170 |
| night | 14 | 32 | 23.0 | 7.1 | 0 | 78 | 28.8 | -0.86 | 0.00 | 0.46 | 89 | 0 | 122 |
| night | 15 | 43 | 22.3 | 5.4 | 0 | 69 | 47.3 | -0.99 | 0.00 | 0.47 | 87 | 0 | 261 |
| night | 16 | 24 | 23.6 | 19.6 | 0 | 67 | 20.4 | -0.15 | 0.00 | 0.39 | 99 | 0 | 31 |
| ctnit | 02 | 23 | 11.5 | 7.3 | 68 | 8 | 1.0 | 3.27 | 0.00 | 0.34 | 15 | 0 | 4 |
| ctnit | 03 | 23 | 11.5 | 10.2 | 58 | 18 | 4.4 | 0.87 | 0.00 | 0.29 | 80 | 0 | 13 |
| ctnit | 12 | 24 | 23.6 | 11.1 | 0 | 86 | 30.9 | -7.29 | 0.00 | 0.40 | 35 | 0 | 83 |
| ctnit | 16 | 24 | 23.6 | 19.6 | 0 | 67 | 6.7 | 1.38 | 0.00 | 0.35 | 74 | 0 | 10 |

det = 3  wvl = 3914 A

| illum | scene | day | lmt | amp | pcsl | pcau | C01 | Cp | Cs | sg0 | pcvf | pcvx | Ray |
|---|---|---|---|---|---|---|---|---|---|---|---|---|---|
| night | 11 | 25 | 23.5 | 13.4 | 0 | 98 | 20.5 | 0.16 | 0.00 | 0.13 | 95 | 0 | 490 |
| night | 12 | 24 | 23.6 | 10.2 | 0 | 106 | 31.1 | -0.35 | 0.00 | 0.24 | 92 | 0 | 975 |
| night | 13 | 29 | 23.3 | 3.6 | 0 | 111 | 9.6 | -0.13 | 0.00 | 0.28 | 99 | 0 | 841 |
| night | 14 | 32 | 23.0 | 4.1 | 0 | 100 | 9.3 | 0.98 | 0.00 | 0.37 | 75 | 0 | 720 |
| night | 15 | 43 | 22.3 | 5.3 | 0 | 92 | 47.3 | -0.80 | 0.00 | 0.28 | 71 | 0 | 2852 |
| ctnit | 11 | 25 | 23.5 | 13.4 | 0 | 98 | 16.5 | .56 | 0.00 | 0.05 | 83 | 0 | 393 |
| ctnit | 12 | 24 | 23.6 | 10.2 | 0 | 106 | 31.4 | -1.73 | 0.00 | 0.13 | 36 | 0 | 986 |

Table 6

det = 1 wvl = 1596 A

| illum | scene | day | lmt | amp | pcsl | pcau | C01 | Cp | Cs | sg0 | pcvf | pcvx | Ray |
|---|---|---|---|---|---|---|---|---|---|---|---|---|---|
| day | 02 | 23 | 11.5 | 85.0 | 67 | 16 | 106.1 | 0.95 | 1.03 | 0.22 | 27 | 30 | 112 |
| day | 04 | 42 | 10.2 | 85.0 | 91 | 15 | 97.6 | 0.89 | 0.95 | 0.23 | 24 | 27 | 103 |
| day | 05 | 43 | 10.1 | 85.0 | 73 | 12 | 59.8 | 0.91 | 0.49 | 0.21 | 30 | 36 | 63 |
| day | 06 | 47 | 9.9 | 51.0 | 75 | 20 | 60.3 | 0.81 | 0.95 | 0.21 | 17 | 21 | 106 |
| day | 07 | 48 | 9.8 | 85.0 | 79 | 25 | 108.5 | 0.85 | 0.98 | 0.24 | 34 | 37 | 114 |
| day | 08 | 55 | 9.3 | 63.8 | 82 | 22 | 85.1 | 0.76 | 0.81 | 0.23 | 38 | 43 | 120 |
| night | 05 | 43 | 10.1 | 85.0 | 73 | 12 | 2.5 | 0.99 | 0.00 | 0.09 | 43 | 0 | 2 |
| night | 07 | 48 | 9.8 | 85.0 | 79 | 25 | 1.9 | 2.57 | 0.00 | 0.39 | 14 | 0 | 2 |
| night | 08 | 55 | 9.3 | 63.8 | 82 | 22 | 2.2 | 1.03 | 0.00 | 0.11 | 43 | 0 | 3 |
| ctnit | 02 | 23 | 11.5 | 85.0 | 67 | 16 | 3.4 | 1.60 | 0.00 | 0.21 | 26 | 0 | 3 |
| ctnit | 12 | 24 | 23.6 | 85.0 | 0 | 114 | 16.8 | -3.53 | 0.00 | 0.30 | 47 | 0 | 17 |

det = 2 wvl = 1356 A

| illum | scene | day | lmt | amp | pcsl | pcau | C01 | Cp | Cs | sg0 | pcvf | pcvx | Ray |
|---|---|---|---|---|---|---|---|---|---|---|---|---|---|
| day | 02 | 23 | 11.5 | 7.3 | 68 | 8 | 128.5 | 0.90 | 0.85 | 0.18 | 4 | 6 | 528 |
| day | 03 | 23 | 11.5 | 10.2 | 58 | 18 | 229.7 | 0.82 | 0.99 | 0.16 | 9 | 14 | 675 |
| day | 04 | 42 | 10.2 | 6.7 | 91 | 8 | 114.1 | 0.93 | 0.98 | 0.21 | 3 | 4 | 510 |
| day | 05 | 43 | 10.1 | 7.3 | 74 | 7 | 90.1 | 0.96 | 0.80 | 0.20 | 6 | 6 | 370 |
| day | 06 | 47 | 9.9 | 5.7 | 75 | 14 | 140.4 | 0.89 | 1.21 | 0.22 | 2 | 3 | 742 |
| day | 07 | 48 | 9.8 | 6.5 | 78 | 16 | 110.9 | 0.96 | 1.02 | 0.21 | 5 | 5 | 508 |
| day | 08 | 55 | 9.3 | 6.4 | 81 | 12 | 93.4 | 0.92 | 0.82 | 0.21 | 4 | 5 | 439 |
| night | 07 | 48 | 9.8 | 6.5 | 78 | 16 | 1.6 | 2.65 | 0.00 | 0.31 | 21 | 0 | 7 |
| ctnit | 02 | 23 | 11.5 | 7.3 | 68 | 8 | 1.0 | 3.27 | 0.00 | 0.34 | 15 | 0 | 4 |
| ctnit | 12 | 24 | 23.6 | 11.1 | 0 | 86 | 30.9 | -7.29 | 0.00 | 0.40 | 35 | 0 | 83 |

det = 3 wvl = 3914 A

| illum | scene | day | lmt | amp | pcsl | pcau | C01 | Cp | Cs | sg0 | pcvf | pcvx | Ray |
|---|---|---|---|---|---|---|---|---|---|---|---|---|---|
| ctnit | 12 | 24 | 23.6 | 10.2 | 0 | 106 | 31.4 | -1.73 | 0.00 | 0.13 | 36 | 0 | 986 |

## 7.2 Aurora

Figure 8 examines two auroral images with respect to two geomagnetic coordinate systems. Magnetic local noon is up in all of Fig. 8 and 9 images. Figures 8a and 8b show aur072.1 and aur152 respectively plotted on a dipole geomagnetic grid. Figures 8c and 8d show the same images on a corrected geomagnetic grid. Aur072.1, which belongs to scene 07, is mostly a daytime aurora. Aur152.1 (scene 15) is a nighttime aurora.

We used the corrected geomagnetic system developed by G. Gustafsson (Ref. 13). It is derived by a perturbation method to calculate the field lines, based on the first seven harmonic terms of the geomagnetic field for epoch 1945.

Figures 8c and 8d entail a comparison of the observed aurora with Feldstein's auroral oval (Ref. 9) for magnetic activity index Q = 3. Note, however, that the oval was originally drawn on a corrected geomagnetic grid with allowance for only the first four harmonics of the internal geomagnetic field expansion. Hence a discrepancy of about 1 degree ( c100 km ) may exist between the grid and the oval.

Figure 9 offers a summary of the 13 scenes processed so far with regard to auroral occurrence around the northern magnetic pole. Figure 9a, 9b, and 9c correspond to auroral images produced bydetector 1, 2, and 3 respectively.

Some basic features of the visual auroral oval parallel the UV ovals of Figures 8 and 9 :

(a) The auroral band is located at lower latitudes ob the nightside compared with the dayside.
(b) The band is broader in the nightside sector compared with the dayside sector.
(c) The global aurora is a closed band encircling the geomagnetic pole.

The observed ultraviolet aurora is in general coincident with the auroral oval. There is, however, a strong discrepancy between Feldstein's oval and our results in the dayside sector. The discrepancy is quite pronounce in Figures 8c, 9a, and 9b. An up to 5 degrees latitudnal deviation exists between the auroral arc and the oval. This dayside anomaly of our auroral images is currently under investigation.

## 8. References


1. Mens, C-I. and Huffman, R. E. (April 1984) Ultraviolet Imaging From Space of the Aurora Under Full Sunlight, Geophys. Res. Lett, Vol 11, #4, pp 315-319.

2. Huffman, R. E. and Mens, C-I. (Apr-Jun 1984) Ultraviolet Imaging of Sunlit Auroras From HILAT, John Hopkins APL Technical Digest, Vol 5, #2, pp 138-142.

3. Huffman, R. E., Larrabee, J. C. and LeBlanc, F. J. (1985) Ultraviolet Remote Sensing of the Aurora and Ionosphere for $C^3I$ System Use, Radio Science, Vol 20, #3, pp 425-430.

4. Schenkel, F. W., Ogorzalek, B. S., Larrabee, J. C., LeBlanc, F. J. and Huffman, R. E. (Oct 1985) Ultraviolet Daytime Auroral and Ionospheric Imaging From space, Applied Optics, Vol 24, #20.

5. Rosenberg, N. (Sep 1986) Computational Physics, Inc.

6. Rosenberg, N. (Sep 1987) Satellite UV Imaging Processing, AFGL-TR-87-0271, ADA190466.

7. Swider, W. J. (1964) Termination of the Optical Depth at Large Solar Zenith Distances, Planet. Space Sci., Vol 12, pp 761-782.

8. Wilkes, M. V. (1954) A Table of Chapman's Grazing Incidence Integral Ch(x,X) Proc. Phys. Soc, B67, pp 304-308.

9. Chapman, B. S. (1931) The Absorption and Dissociative or Ionizing Effect of Monochromatic Radiation in an Atmosphere on a Rotating Earth. Part II. Grazing Incidence, Proc. Phys. Soc., Vol 43, pp 26-45 and 483-501.

10. Feldstein, Y. I. and Starkov, G. V. (1967) Dynamics of Auroral Belt and Polar Geomagnetic Disturbances, Planet. Space Sci., Vol 15, #2, pp 209-229.

11. Akasofu, S-I. and Chapman, C. (1972) An Account of the Wave and Particle Radiations From the Quiet and the Active Sun, and of the Consequent Terrestrial Phenomena, Solar Terrestrial Physics, Fig. 8.54.

12. Feldstein, Y. I. and Galperin, Yu. I. (1985) The Auroral Luminosity Structure in the High-Latitude Upper Atmosphere: Its Dynamics and Relationship to the Large-Scale Structure of the Earth's Magnetosphere, Rev. Geophys., Vol 23, #3, pp 217-275.

13. Gustafsson, G. (1969) A Revised Corrected Geomagnetic Coordinate System, Arkiv for Geofysik, Vol 5, pp 595-617.

## Appendix 1

### Geometric processing

1a. rawcvt help :

```
USAGE  rawcvt SYYDDD NND (raW bsB esF ssS fsS lpL hpH) < ASCI
EXAM   rawcvt  S86338 011 < A:S87008h2.dat
INPUTS   ASCI file with original BC file format
OUTPUT   air/rawNND.1, rawNN.d if doesn't exist, else check vs air/rawNN.d
         image qd=2 xfered to qd=1 (rot if necessary)
SYYDDD  converted in rawfit to site, yr and day
NND     air code (scene) and detector : D => 1 = 1596A, 2 = 1356A
         3 = 3914A, 4 = 1733A, 5 = 1493A, 6 = 1544A, 7 = 1304A
stretches input to image (240 line x 240 col)
estimates lines from file header start and final sec
  if conflict report start and final sec in line hdr
  can rerun with options ssS and fsS described below
options if present
  raW W=1 output ql raw data 326 cols x input lines (no output of rawNND.1)
  bsB flags begin sec for image (if bad section)
  esE flags end   sec for image (if bad section)
  ssS S= start sec to override header start sec error
  fsS S= final sec to override header final sec error
  lpL hpH low high input kol with non-zero (def=5 330)
  bgB B=2 quits after hdr read
```

1b. scene help :

```
USAGE  scene NN (aim nrR lmH ksK fdG dtD)
EXAM   scene 03
 INPUTS   air/rawNN.d, air/rawNND.1
 OUTPUTS  air/hdrNN.d, air/geoNN.d, air/selNN.1
  NN = scene number; D = detector number
options
  aim for aim images (def : air)
  nrR R=1 for no roll adjustment
  lmH H=  limb height in kilometers
  ksK K=0 or 239; column to start search brightest limb from
  fdG G=1, 2,.. ; polynom degree for roladj collumn fit
  dtD D=1, 2, or 3; rawNND.1 to choose for roladj calc
defaults: nr0 lm150 fd0 (G=0 no fit - continous search)
          ks = automatic choice ( side closest to sun )
          dt = automatic choice ( most sensitive detector )
EXAM   scene 11 ks239 fd3 dt3
```

1b. scene 11 output :

rawfit
---

```
   fit  G = ground km along path to GO + VEL*(TIM-TIM0)
   calculated velocity:    6.38 +- 0.006 km/sec
   zero ground range:      2.87 km

   data reversed to north
```

roladj
---

```
   uses image raw113.1 to find roll adjustment
   sunlit side of image is not the brightest
   brightest col = 239, sunlit col =   0
   start searching brightest limb from column 239

   line  0: roll adjustement =  4.4 degrees
   line 10: roll adjustement =  3.9 degrees
   line 20: roll adjustement =  3.3 degrees
   line 30: roll adjustement =  5.5 degrees
   line 40: roll adjustement =  6.1 degrees
   mean roll adjustment for 0 lines = 4.3 +- 1.3 degrees
```

geomim
---

| left | right | x | | | | y | |
|---|---|---|---|---|---|---|---|
| -64.3 | 55.7 | 5 | 1 | -1 | -1950 | 60 | 1950 |
| -63.2 | 56.8 | 914 | 910 | 907 | -1946 | 45 | 1946 |
| -65.2 | 54.1 | 1823 | 1819 | 1817 | -1812 | 84 | 1944 |

solel
---

| latitude | | | longitude | | |
|---|---|---|---|---|---|
| 69.4 | 77.6 | 68.7 | 204.7 | 237.4 | 42.8 |
| 63.9 | 69.5 | 63.3 | 218.7 | 262.5 | 359.2 |
| 57.7 | 61.3 | 56.8 | 229.0 | 261.5 | 344.9 |

```
 latitude and longitude of solar noon      =  -19.8, 147.1
 solar elevation (degress) in image center =  -42.2
```

warpim
---

# Appendix 2

## Photometric processing

### 2a. detc help :

```
USAGE detc NND  (aim nwN wwW nsM stA pcU)
EXAM detc 122
 INPUTS   air/hdrNN.d, air/geoNN.d, air/rawNND.1
 OUTPUTS  air/hdrNN.d, air/warpNND.1
  NN = scene number; D = detector number
options :
  aim for aim images (def: air)
  nwN N = narrow width smoothing (def: automatic select)
  wwN N = wide  width  smoothing (def: automatic select)
  nsM M = number of smooths
  stA A = 1 amplify airglow to 200 (saturate aurora)
  pcU U = percent aurora (def: automatic selection)
defaults: nw3  ww19  ns1  st0
EXAM  detc 022 nw2 ww23 ns3 st1
```

detc 072 ouput :

```
filtraw
-------
 # pixels mod-smoothed = 0
percent aurora from raw modeling = 21
 average auroral signal =  17.7  ==> using smoothing width  3 pixels wide
 average airglow signal =   3.5  ==> using smoothing width 19 pixels wide
 smoothing 1 times
 average input  signal =    6.20
 average output signal =   41.11
 amplification         =    6.54

warpim
------
image  size   = 5000 km    pixel  size   =   21 km
north  center = 2189 km    east  center  =  -31 km
line   center =  105       column center =   -1


hdr07.d contents :
---------------
AIR     07
Site   SON        LMTC     9.8
Year    87        Linp   239
 Day    48        LatC    68.4
GMTC   14.4       LonC   291.5
 Dir     S        Detc       1       2
SelC     8.0      Wvlg    1596    1356
StmC    11.3      Rpau      27      21
RStC     3.3      Ampk   85.00    6.54
Radj     1.5      Pcsl      79      78
Upak    NO        Pcau      25      16
```

2b. geomlsq help :

```
USAGE     geomlsq NNN (aim loB plP)
INPUTS    air/warpNNN.i, air/selNN.i, air/hdrNN.d
OUTPUT    air/aurNNN.i, air/hdrNN.d
  NN = scene number, D = detector number (air images only)
  aim to deal with aim images
  plP limit analysis to inv path length of counts > P
  loB do not use inputs less than B
defaults : air lo3 pl50 (path <= 4)
EXAM geomlsq 042
```

geomlsq 072 output :

```
limit inverse path length to count >= 50, i.e. to pl <= 4.0
lowest brightness for fit: lo_b = 3
limit lsq fit to day sinselv >= 121 and night sinselv <= 82
totdk 8380 totsl 32764 tot 41144
p_mn 12 p_mx 201 s_mn 1 s_mx 110  pcsl 80
total data points for analysis  =   9500
```

| | (lg)C0 | sdv0 | sdvf | pcvr | C01 | Cp | Cs | pcsd | pts |
|---|---|---|---|---|---|---|---|---|---|
| fxc sl | 2.03 | 0.13 | 0.05 | 13 | 107.80 | -1.00 | 1.00 | 11 | 2209 |
| fxc sl | 2.03 | 0.22 | 0.05 | 5 | 106.14 | -1.00 | 1.00 | 11 | 3401 |
| nfc sl | 2.03 | 0.13 | 0.05 | 12 | 99.41 | -0.93 | 0.92 | 11 | 2209 |
| nfc sl | 1.90 | 0.21 | 0.04 | 5 | 110.92 | -0.96 | 1.02 | 11 | 3270 |
| nfc dk | 7.98 | 0.25 | 0.23 | 85 | 0.80 | -3.51 | 0.00 | 70 | 84 |
| nfc dk | 6.30 | 0.31 | 0.14 | 21 | 1.62 | -2.65 | 0.00 | 40 | 479 |

```
 reimaging with aurora threshold =  47
 and with sigma threshold in day = 220, at night = 179, in 24hr night =  0
```

| source | npts | av | sg | med | i99 | pc_sg/av |
|---|---|---|---|---|---|---|
| slbr | 25406 | 52.4 | 36.5 | 41 | 179 | 69 |
| dkbr | 5530 | 20.3 | 19.5 | 13 | 86 | 96 |
| dkcb | 1799 | 2.9 | 3.0 | 1 | 15 | 104 |
| slft | 25401 | 126.4 | 41.6 | 110 | 239 | 32 |
| dkft | 5521 | 129.3 | 62.9 | 114 | 239 | 48 |
| dkcf | 1799 | 2.9 | 3.0 | 1 | 15 | 104 |
| aubr | 5351 | 86.1 | 27.6 | 79 | 185 | 32 |

```
opens air/hdr07.d for update
creats air/lsq072.d for output
```

## Appendix 3

### Coordinate systems

3a. landmass help :

```
USAGE landmass (qQ nN (eE or wW) aNN kK dD rR oO gG sS pP mM cC bB hH vV)
options
qQ output quad 1-4 (def 1)
nN = ctr_lat eE = ctr_lon kK = km_wide (def = 5000 km)
EXAM landmass n54.5 w85.2
aNN  gets N and E from air/hdrNN.d file
pP proj 1 = view from inf  2 = from ecen aong orbit (2 = default)
        3 = sphere 4 = hemisph  5 = Mercator
xX X = 0: no cross at image center; 1,2,...: cross of size 12/X (def: X = 2)
cC C = 1 clears screen before run ( default: C = 0 )
oO rotate for O  =  90 deg - orbital_angle
dD lat lon  point spacing (def 6)
gG land-mass point spacing (def 2)
sS = min segment pts for lndmass(def = 50 0 = all)
mM mesh for interp (def = 14 max = 20)
lL color of landmasses def = 180
hH vV horiz vert points  def 240 240
zZ overlay km grid
rR R = 1 grid lat/lon only R =  -1 landmass only
input files: data/worlb.d binary generated from worsort


landmass alb output :

hdrlb lat = 69.8 lon = 31.8
qo = 1 latc =  69.8 lonc =   31.8 kmw =   5000
proj = 2 mesh = 14 orb =   0.0 qsp = 2  spts = 50
lat mn mx range  35  90   55 lon mn mx range -180 180 180
maps lamn lamx lomn lomx  35    90  -180   180
```

3b. aurplot help :

```
aurplot NND ( scS ncl dip nolat orig pole )
   NN: scene  number, D: detector number (e.g. 072)
    S: screen number (def: S = 20, options = 0,10,20,30)
  ncl: do not clear total screen before plotting (def: clear)
  dip: plot dipole coordinates (def: corrected coord.)
nolat: no plotting of latitude reference lines (def:plot)
 orig: plot original aurora on upper left side of screen (def:no)
 pole: find geographic coord of image point closest to magnetic pole (def:no)
```

```
aurplot 152 output :

latitude of sun:  13.9
longitude of sun: 163.5

geomagnetic latitude of sun:    8.6
geomagnetic longitude of sun: 231.6

latitude of magnetic pole:  78.7
longitude of magnetic pole: 279.5


3c.  gmcoord help :

gmcoord NN  ( gg gm dip scS qdD cl nnum flatDD llatDD ilatDD flonDD llonDD il

   NN: scene number
    gg: plot geographic coordinates or
    gm: plot corrected geomagnetic coordinates or
   dip: plot dipole geomagnetic coordinates
     S: screen number (def: 10)
     D: quadrant number (def: 1)
    cl: clear screen before displaying (def: no)
  nnum: do not display coordinate values (def: display)
  flat: first latitude value to plot (def: picture values)
  llat: last latitude value to plot (def: 85 deg)
  ilat: latitude increments to plot (def: 5 deg)
  flon: first longitude value to plot (def: 0 deg)
  llon: last longitude value to plot (def: 360 deg)
  ilon: longitude increments to plot (def: 20 deg)


gmcoord 07 dip output :

latitude of sun:   11.9
longitude of sun: 324.0
geomagnetic latitude of sun:  21.4
geomagnetic longitude of sun: 34.9
latitude of magnetic pole:   78.2
longitude of magnetic pole: 291.1


3d.  aurmean help :

aurmean  NND  ( dip rem dis ncl )
  dip: calculate dipole coordinates (default: corrected coord.)
  rem: remove the specified image from file (def: add)
  dis: display D aurora contents - use aurmean 00D dis (def: no)
  ncl: no clear screen (def: yes)

aurmean 001 dis output :

  detector number  : 2
  coordinate type  : corrected geomagnetic
  processed images : 2 3 4 5 6 7 8 11 12 13 14 15 16
```

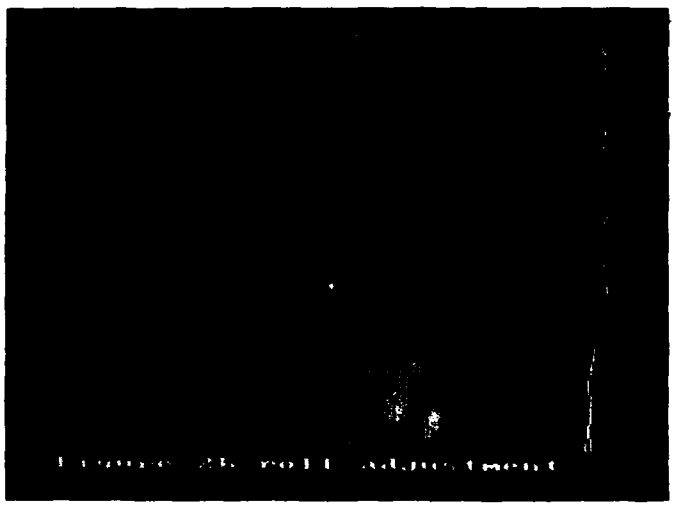

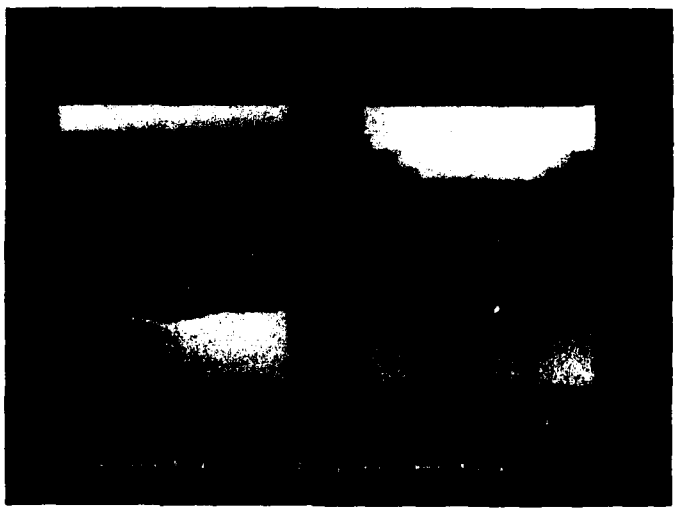

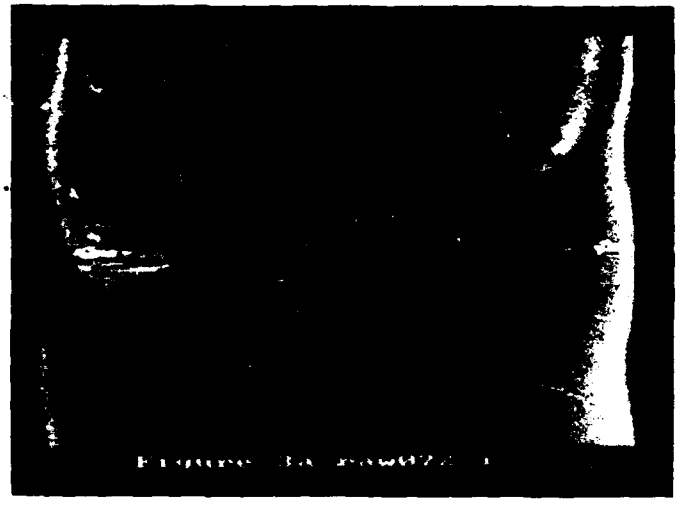

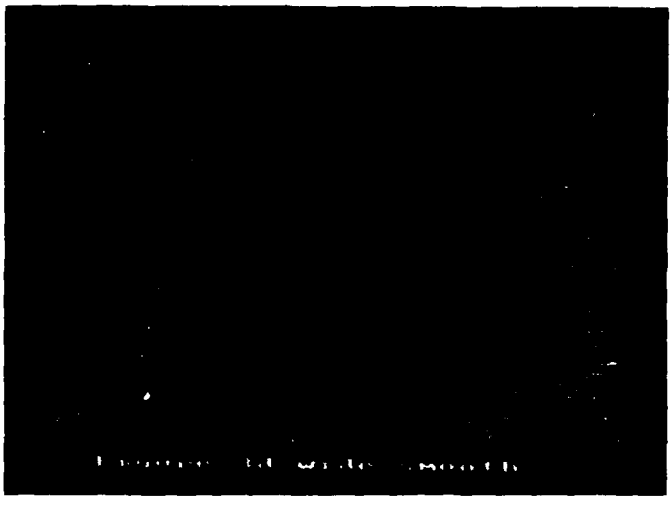

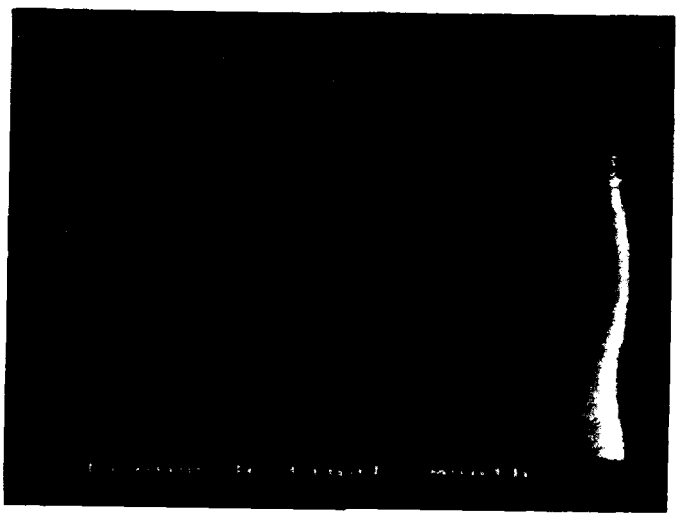

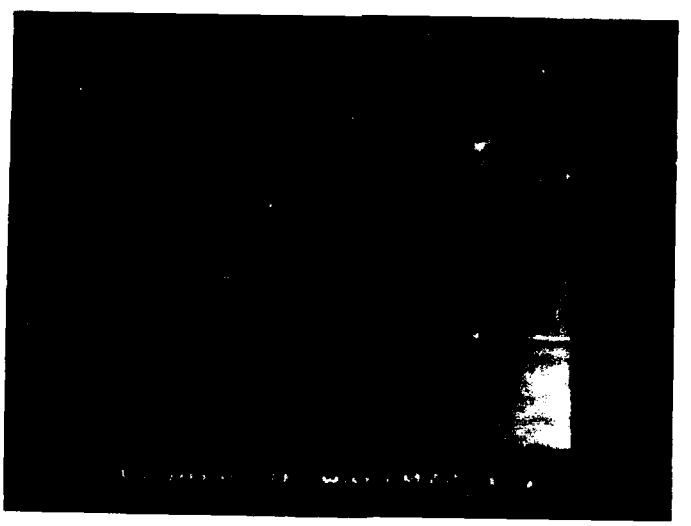

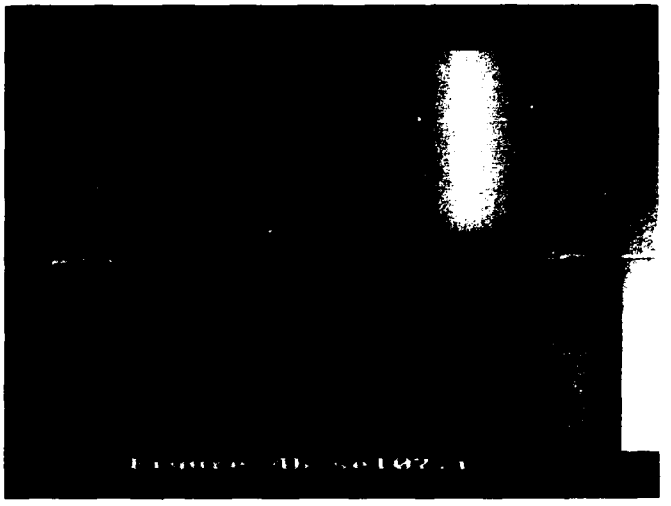

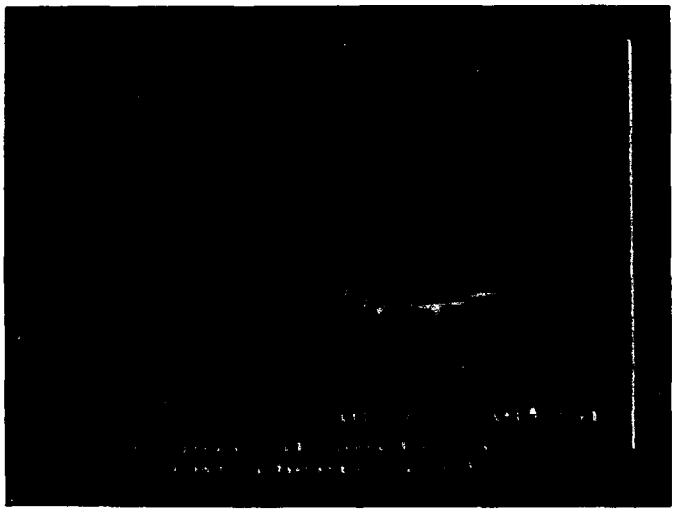

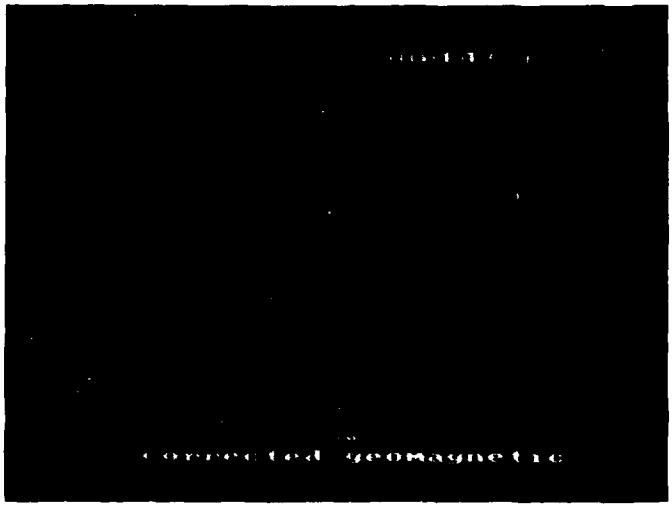

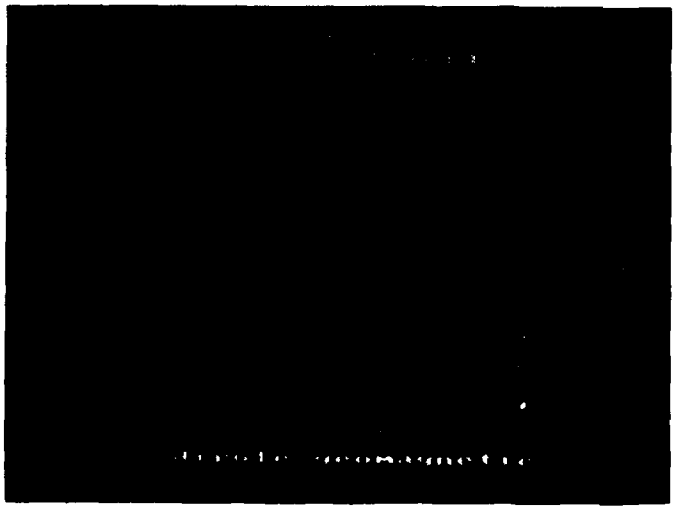

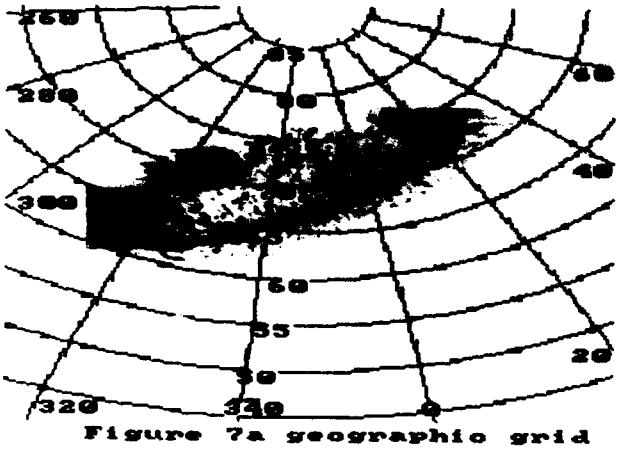


Figure 7a geographic grid

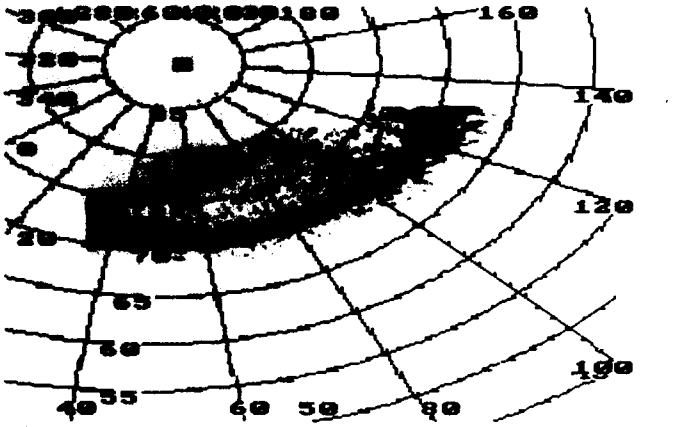


Figure 7b corrected geomagnetic

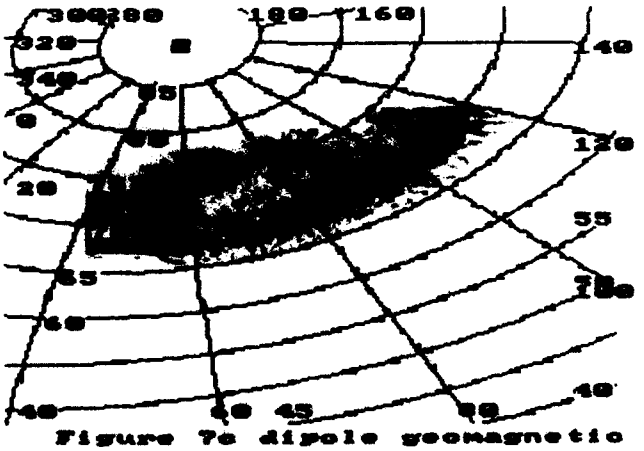


Figure 7c dipole geomagnetic

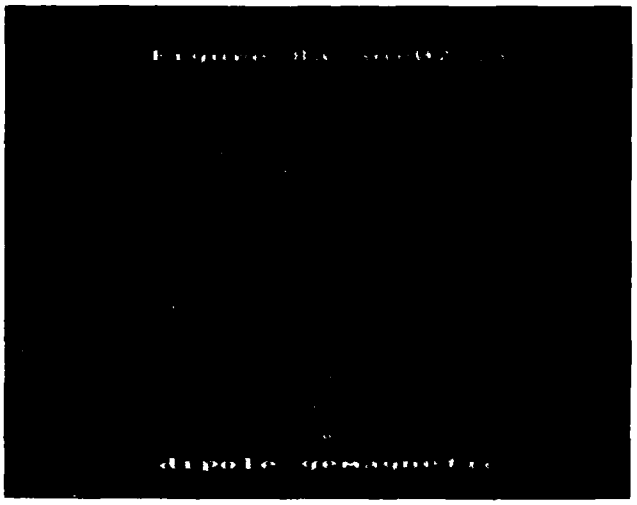
dipole geomagnetic


dipole geomagnetic

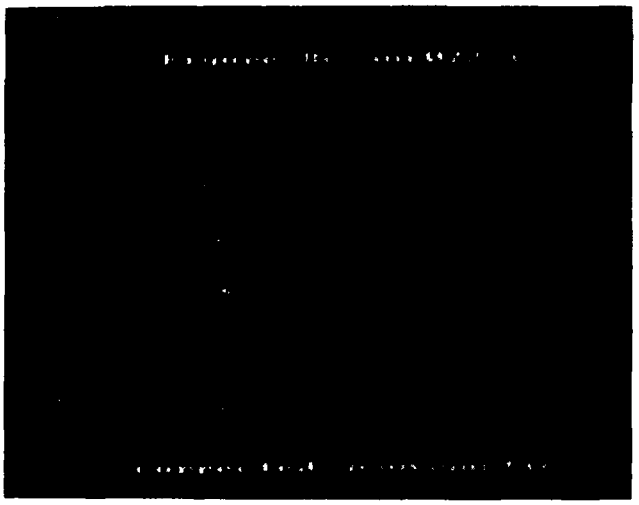

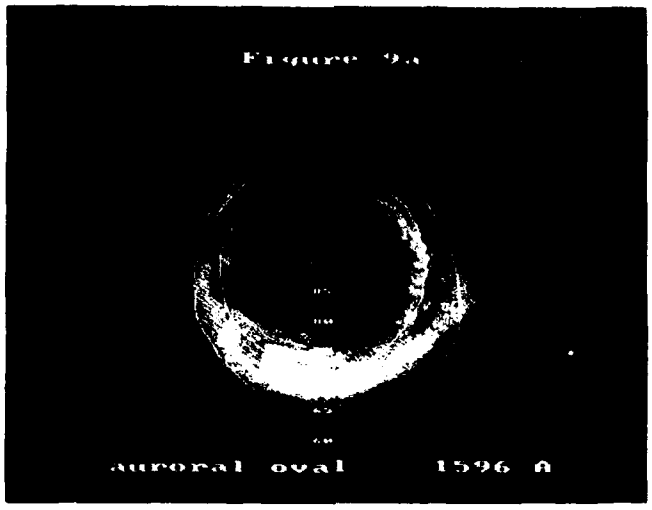
auroral oval 1596 Å

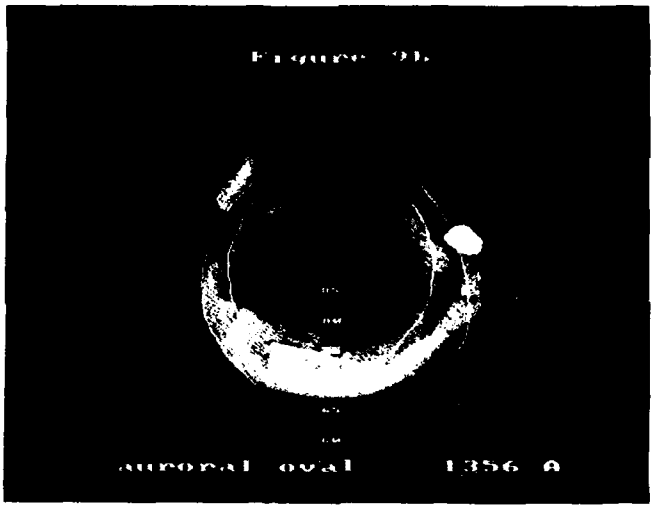
auroral oval 1356 Å

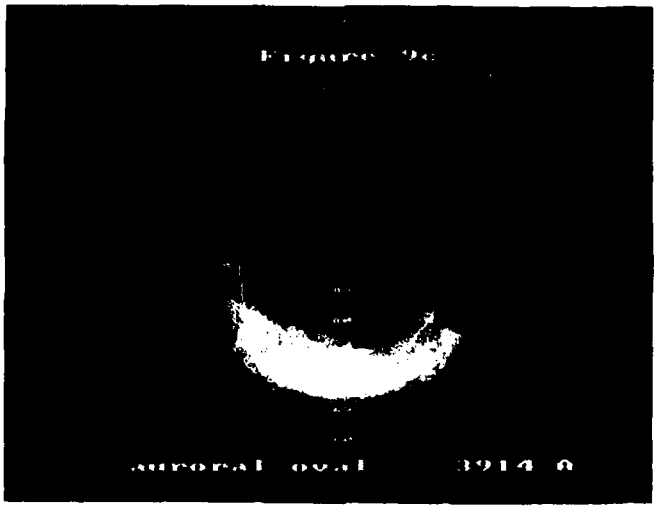
auroral oval 3914 Å